Cell Reports
Physical Science

CellPress
OPEN ACCESS

Article

Direct capture of carbon dioxide from the atmosphere using bricks of calcium hydroxide

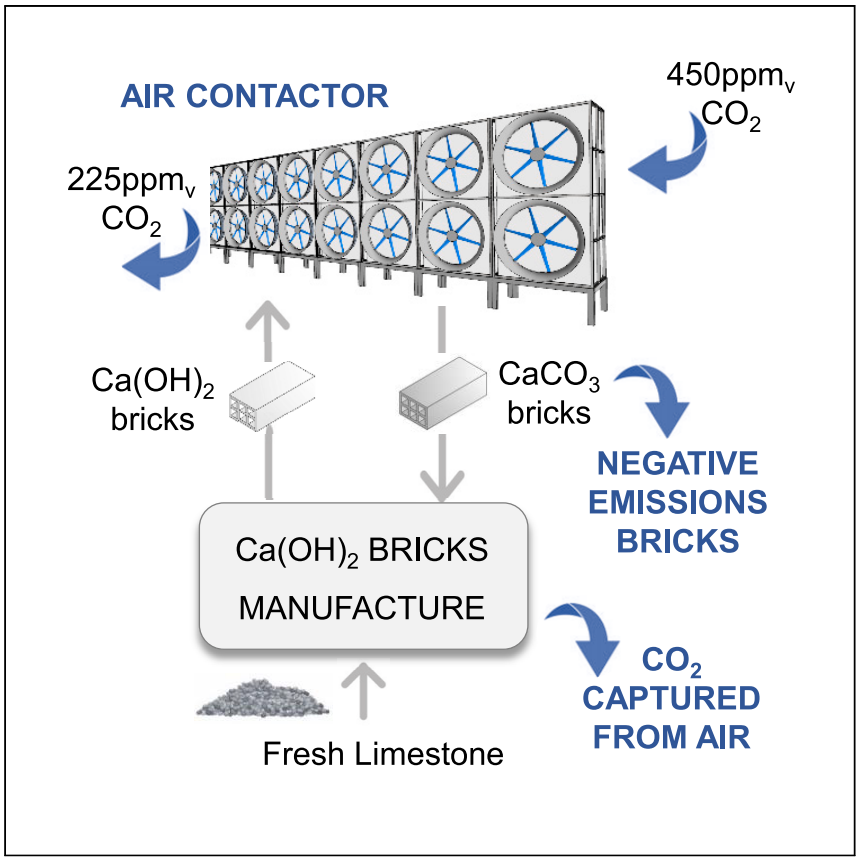

Abanades et al. present a DAC system where bricks manufactured from a dry lime mortar are carbonated in contact with air. The bricks can then be destroyed and recycled using mature technologies to extract the captured CO_2 at a competitive cost compared with other DAC alternatives.

J. Carlos Abanades, Yolanda A. Criado, Heidi I. White

yolanda.ac@incar.csic.es

Highlights

Design and cost analysis of a 1 Mt-CO_2/year DAC system

Contactor based on porous $Ca(OH)_2$ bricks aligned to accommodate an induced air flow

Brick production/regeneration based on emerging and standard industrial operations

DAC cost (without contingencies) are between 131 and 251 \$/t-CO_2

Abanades et al., Cell Reports Physical Science 4, 101339
April 19, 2023
https://doi.org/10.1016/j.xcrp.2023.101339

Cell Reports
Physical Science

CellPress
OPEN ACCESS

Article

Direct capture of carbon dioxide from the atmosphere using bricks of calcium hydroxide

J. Carlos Abanades,[1] Yolanda A. Criado,[1,2,*] and Heidi I. White[1]

SUMMARY

Direct air capture (DAC) of CO_2 plays a key role in most 1.5°C climate scenarios. The low concentration of CO_2 in ambient air results in high contactor volumes, air flow rates, and energy requirements. Here, we investigate a DAC system based on the carbonation of $Ca(OH)_2$ hollow bricks piled in stacks that move counter-currently with respect to the air flow. Capture efficiencies of 50% can be obtained with a contactor approximately 10 m deep, with a pressure drop below 200 Pa at air velocities of 3–4 m/s inside the brick holes. To capture 1 Mt-CO_2/year, DAC cost approaches 251 and 131 $/t-$CO_2$ (without contingencies) for a first and an n^{th}-of-a-kind system, respectively, relying on emerging technologies to decarbonize the lime and cement industries. If the carbonated bricks find a value as construction materials, breakthrough decreases in costs can be achieved.

INTRODUCTION

Negative emissions technologies are required in all scenarios compatible with limiting global warming to +1.5°C by the end of the century.[1,2] Direct air capture (DAC) of CO_2 is considered to be a negative emissions technology when combined with permanent storage of the captured CO_2 (DACCS).[3–7] DAC is also able to provide a sustainable source of CO_2 for the manufacture of synthetic fuels, thus making them truly carbon neutral when produced using carbon-free renewable energy.[8–11]

Most developed DAC systems are based on the use of hydroxide or amine liquid solvents or in sorbent processes using functionalized solid materials.[6] DAC technology has been developed up to TRL6, with Carbon Engineering (www.carbonengineering.com), Climeworks (www.climeworks.com), and Global Thermostat (www.globalthermostat.com) as leading companies. Between them, 18 pilot plants are in operation, capturing a total of 8,000 t-CO_2/year and with individual capacities of up to 4,000 t-CO_2/year (www.carbfix.com). One-half of the total CO_2 captured is stored permanently, and the rest used for industrial applications, agriculture, and the synthesis of carbon-neutral fuels. It has been announced recently that the Carbon Engineering DAC system[12] will reach commercial scale by late 2024, capturing at a rate of 1 Mt-CO_2/year (www.1pointfive.com). Several studies indicate that more than 100 of these DAC facilities are expected to be deployed within the next decade (see for example, www.carbonengineering.com, www.1pointfive.com, and www.oxy.com). In addition to the Carbon Engineering DAC system, industrial-scale demonstration projects with ambitious scale-up plans for solid-sorbent-based DAC systems are under development.[3,4] Research into advanced functional materials is also expanding rapidly,[4,13] as decreases in sorbent costs and improved performance will be critical for the

[1]CSIC-INCAR, C/ Francisco Pintado Fe, 26, 33011 Oviedo, Spain

[2]Lead contact

*Correspondence: yolanda.ac@incar.csic.es

https://doi.org/10.1016/j.xcrp.2023.101339

deployment of these sorbent-based systems. Despite current limitations on sorbent cost and performance, Climeworks expect to achieve the megaton scale for CO_2 capture by 2030 and the gigaton scale by 2050.[14] Also, the Haru-Oni project (www.haruoni.com) aims to manufacture 1 Mt/year of green methanol by 2026 from green H_2 and CO_2 captured form air using Global Thermostat DAC technology.

Early cost analyses suggested total DACCS system costs on the order of 1,000 \$/t-CO_2.[15] However, in a recent International Energy Agency Greenhouse Gas R&D Programme (IEAGHG) report on DACCS,[16] it has been concluded that total costs of first-of-a-kind DACCS projects are likely to range from 300 to 600 \$/t-CO_2 captured. Energy consumption ranges from 5 to 11 GJ/t-CO_2 for thermal needs and from 0.6 to 9 GJ/t-CO_2 for electrical needs in current DACCS systems,[16] indicating that total cost figures are extremely sensitive to energy costs. Herzog[17] has recently re-assessed the available literature on DAC cost and concluded that reasonable expectations for DAC costs in 2030 remain in the range of \$600–\$1,000 per net t-CO_2 removed. This was assessed after due consideration of major issues, including the availability of low-cost, carbon-free energy for high-capacity factor DAC plants, regulatory and permitting rules, water availability, environmental issues, etc.

The use of $Ca(OH)_2$ in DAC systems is of particular interest for this work. Solutions of $Ca(OH)_2$ in water were considered a suitable solvent for the capture of CO_2 from air at the onset of research into DAC[18–20] and are an essential intermediate product in the Carbon Engineering DAC system.[12] Here, a $Ca(OH)_2$-$CaCO_3$ loop (requiring the oxy-calcination of $CaCO_3$ and a standard hydration process of CaO) is coupled to regenerate the KOH water solution needed to absorb CO_2 and form K_2CO_3 in an air-liquid contactor.

The dry solid form of $Ca(OH)_2$, on the other hand, has been used as a mortar for millennia[21]; it can be easily shaped and does not experience deformation under slow-hardening carbonation in contact with the atmosphere. More recently, the use of porous Ca-based materials as enablers for DAC applications has been investigated.[22–26] Their dry solid forms have been observed to have favorable structural properties,[24] similar to those of other carbonate binders and cementitious materials.[27] We have investigated[25] the disposal of large-scale $Ca(OH)_2$ porous structures to exploit the known passive carbonation phenomena of these materials. In the Calcite project, 8-Rivers[26] will attempt a large-scale demonstration of a novel DAC system that uses thin layers of $Ca(OH)_2$ slurry that carbonate when in contact with ambient air. Similarly, Heirloom (www.heirloomcarbon.com) investigates a DAC system based on $Ca(OH)_2$ powder spread onto vertically stacked trays.

In this work, we present a DAC contactor able to capture 1 Mt-CO_2/year by achieving adequate contact between an air flow and an arrangement of brick-like forms of $Ca(OH)_2$ dry mortars. Using cost estimations consistent with similar scale commercial systems for each system component, a transparent value of total DACCS cost is obtained. This cost is shown to be competitive with other DACCS systems. The potential use of the carbonated bricks as construction materials could translate into a breakthrough decrease in capture cost under certain conditions.

RESULTS AND DISCUSSION

Air contactor design

The objective of any DAC contactor is to remove CO_2 from the atmosphere at a scale large enough to provide a meaningful contribution to climate change mitigation, as

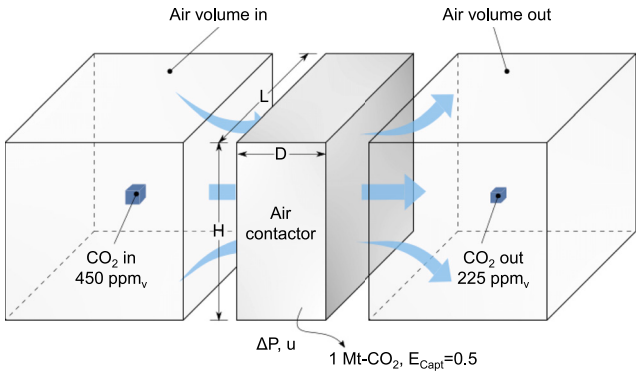

Figure 1. Schematic representation of a generic DAC contactor

This schematic representation highlights the challenge to remove CO_2 from the atmosphere at a rate relevant for climate change mitigation. For a target CO_2 capture rate of 1 Mt-CO_2/year, an assumed capture efficiency of 50% and air at standard conditions with 450 ppm_v CO_2, any DAC contactor needs to treat an air volume of 2.4×10^{12} m^3. This figure also introduces some of the nomenclature used for the design of the air contactor, presented in Table 1 and Figure S1.

illustrated in Figure 1. To remove 1 Mt-CO_2/year from air with a concentration of 450 ppm_v of CO_2 at a capture efficiency of 50%—as adopted in this work as a reference (see Note S1)—requires an air volume of 2.4×10^{12} m^3 to pass through the contactor per year. In the proposed DAC system, the continuous flow of $Ca(OH)_2$ in the form of bricks allows the air contactor to operate in steady state and the bricks to carbonate throughout their residence time in the air contactor volume. For simplicity, this is not represented in Figure 1, but is detailed in Figures S1 and S2.

If the DAC system operates at a 90% capacity factor, the air flow rate through the cross-section HxL approaches 85,600 m^3/s at 20°C. High air velocities, u, will decrease the cross-section, but for any DAC contactor filled with absorption packing elements or solid sorbents, the increase in air velocity will increase the static pressure, ΔP, needed to overcome the total resistance to the air passage through the depth of the air contactor, D. This pressure is typically provided by an array of fans whose electricity consumption can escalate rapidly with u and D, as shown in Note S1 and Figure S3. Therefore, the total electricity consumption of the air fans must be kept within a feasible range and consistent with current estimates for similar parameters in major DAC systems[6,12] (i.e., between 0.22 and 1 GJ_e/t-CO_2, respectively). This imposes a maximum allowable ΔP of 200 Pa for air velocities of 2–2.5 m/s in the cross-section HxL, which is achievable with large-diameter axial fans, such as those found in cooling towers,[28] air-cooled heat exchangers,[29] and other major DAC systems.[3,28]

Another consequence of the low CO_2 concentration in atmospheric air is the very low driving force for the transport of CO_2 from the air toward the gas-solid contacting surface. The carbonation process of porous $Ca(OH)_2$-based materials in contact with ambient air is known to be governed by the gas diffusion of CO_2 through the pores of the $CaCO_3$ product.[30,31] We have recently reported[24] experimental measurements of the carbonation rates of $Ca(OH)_2$ dry mortars with porosities between 0.2 and 0.8 and a thickness between 4 and 15 mm. The model that fits the experimental data is consistent with results from previous researchers investigating the carbonation of other dry porous $Ca(OH)_2$ and Ca-based cementitious materials.[30,31] Furthermore, early studies on the carbonation of $Ca(OH)_2$ under ambient conditions[21,32] highlighted the importance of high levels of humidity in the air feed into

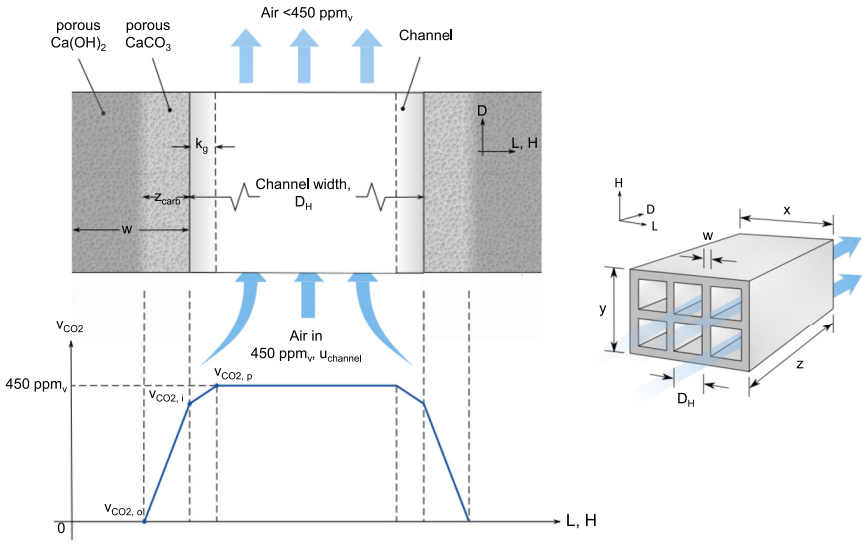

Figure 2. Schematic representation of the CO_2 concentration gradients in the air channels formed by arranging $Ca(OH)_2$ bricks in the air contactor

Extruded hollow bricks with standard dimensions (right) are shown to be viable forms for packaging the dry $Ca(OH)_2$ solids needed in the air contactor, where the air flows through the channels by aligning the bricks as shown in Figure 3. The carbonation of these porous $Ca(OH)_2$ bricks is governed by the gas diffusion of CO_2 through the pores of the formed $CaCO_3$ and the mass transfer in the film of the channels (as shown in the left of the Figure, with mass transfer equations as detailed in Note S1). For this diffusion-controlled model, the CO_2 concentration approaches zero at the boundary between the carbonated material and unconverted $Ca(OH)_2$ (bottom left). This figure also introduces some of the nomenclature used for the carbonation model and the design of the $Ca(OH)_2$ bricks, presented in Table 1 and Figure S1.

the contactor (i.e., relative humidities of greater than 50% and ideally greater than 80% for low surface materials[24]) in ensuring a maximum molar carbonation conversion of $Ca(OH)_2$ to $CaCO_3$ (X_{max} of >0.8).

For the kinetic carbonation model of the $Ca(OH)_2$ bricks mentioned in the previous paragraph, the concentration of CO_2 approaches zero at the boundary between the layer of material already carbonated and the unconverted porous $Ca(OH)_2$. This is represented in Figure 2 (left), along with the mass transfer coefficient (k_g) in the film of the channels, which governs the carbonation of the initial $Ca(OH)_2$ bricks with a zero or negligible porous layer of $CaCO_3$. In Note S1, we describe the sub-model used to estimate carbonation rates (i.e., the rate of advance of the carbonated layer, z_{carb}) as function of the air channel width (D_H), the gas velocity in the channels ($u_{Channel}$), and the geometry of the bricks as represented in Figure 2 (right).

Using the model described in Note S1, it was concluded that a standard brick shape extruded form as shown in Figure 2 (right) (with 8-mm-thick walls separating 27-mm square channels) represents a viable candidate for the porous $Ca(OH)_2$ packing in the air contactor. Its characteristics are detailed in Table 1. Other forms could be adopted (tiles, cylinders, etc.), so long as their geometry enables air flow through the contactor at a sufficiently low ΔP. One possible option is the stacked, vertically spaced plates proposed in a previous study on the passive carbonation process of $Ca(OH)_2$.[25] However, the adoption of standard brick dimensions allows the use of readily available techniques to produce $Ca(OH)_2$ solids forms, which are similar to those already in use in the construction and solid processing industries (see, for example, www.verdes.com). For such forms, a trade-off exists between their

Table 1. Summary of the design choices and calculated parameters of the proposed contactor design

Parameter		Symbol	Value	Units
Design choices				
Target	air contactor capture target	Mt-CO_2/year	1	Mt-CO_2/year
	capture efficiency	E_{Capt}	0.5	–
	capacity factor	CF	90	%
Input air	CO_2 concentration in inlet air	$\nu_{CO2,in}$	450	ppm_v
	inlet air temperature	T_{in}	20	°C
	inlet air relative humidity	RH_{in}	90[a]	%
	superficial air velocity at the exit of the fans	u	2[b]	m/s
Bricks	thickness of bricks wall	w	8[c]	mm
	square channels	D_H	27[c]	mm
	gaps between bricks	D_{gap}	14	mm
	brick dimensions	x•y•z	113•78•250[c]	mm•mm•mm
	brick porosity	ε_{Ca}	0.35[a]	–
	maximum $Ca(OH)_2$ carbonation conversion to $CaCO_3$	X_{max}	0.9[a]	–
	carbonated layer thickness	z_{carb}	3.2	mm
Calculated parameters				
Total flow	volumetric air flow	$Q_{air,\ in}$	85,560	m^3/s
	molar flow of $Ca(OH)_2$ bricks	F_{Ca}	1,090	mol/s
Contactor input air	air velocity in the channels	$u_{Channel}$	3.2	m/s
	static pressure required to overcome the total resistance in the contactor	ΔP	114	Pa
Contactor design	brick residence time	t_R	807	h
	contactor cross-sectional area	HxL	43	ha
	contactor depth	D	10	m
	contactor volume	HxLxD	$4.3 \cdot 10^5$	m^3
	stack volume	V_S	1.8	m^3

The detailed design of the air contactor, based on the plug flow model used to estimate capture efficiencies, can be found in Note S1.

[a]Reference values taken from Criado and Abanades,[24] air flows with modest relative humidity could also be treated when using commercial high-surface $Ca(OH)_2$ porous materials.[24]

[b]Value taken to moderate the static pressure and thus, the fan power consumption.

[c]Values taken from standard bricks for construction applications.

porosity, the initial mechanical properties of $Ca(OH)_2$ bricks, and the final mechanical properties of the carbonated bricks. As discussed in the cost analysis section, the manufacture of $Ca(OH)_2$ forms with suitable dimensions for use in construction applications can satisfy the demand for masonry units manufactured with negative emissions footprints (www.carboncure.com), while decreasing the cost of capturing CO_2 from air. The mechanical properties of the forms leaving the contactor will be enhanced because of the development of a carbonated layer, which is known to increase their crushing strength.[24,33] In addition, the use of cementitious additives and aggregates for enhanced mechanical properties, as needed for construction applications, is an open research topic for this system.

To moderate the residence time of the $Ca(OH)_2$ bricks in the air contactor and, therefore, minimize the air contactor volume and depth, the maximum thickness of the carbonated layer (z_{carb}) can be made lower than the characteristic thickness of the brick walls, w. In other words, it is not necessary that the bricks are fully carbonated during their passage through the air contactor. Favorable mechanical properties arise even when only a fraction of the thickness is carbonated. This could translate to a large decrease in air contactor volume with respect to any other air contactor system. However, since the experimental information relating z_{carb} with brick mechanical properties is limited,[24] and to facilitate comparison with cost figures from other DAC systems, we have adopted a high

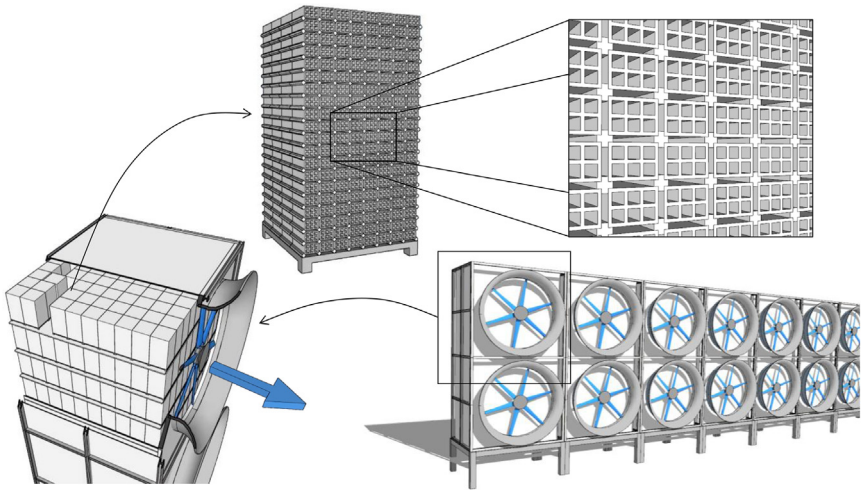

Figure 3. Overview of the air contactor proposed to carbonate the $Ca(OH)_2$ bricks capturing CO_2 directly from air

Front and detailed views of a section of the air contactor (right and left bottom, respectively). This includes the array of axial fans required to overcome the resistance to the air passage through the contactor depth and the arrangement of bricks in stacks (top views). The average movement of the bricks in the contactor is facilitated by the intermittent displacement of stacks of bricks, as shown in the bottom left. To ensure a homogeneous supply of CO_2 to the exposed solid surfaces of the bricks, the bricks holes are aligned, and gaps between bricks are incorporated, as detailed in the top right.

value of z_{carb} (80% of the maximum) for the conversion of the bricks inside the air contactor.

The brick dimensions adopted in Table 1 allow the packing of the bricks in stacks with their holes aligned to form an arrangement of air channels, facilitating the passage of the air through the air contactor. The overall setup of the contactor is presented in Figure 3. For the reference case adopted, the contactor volume is $4.3 \cdot 10^5$ m^3 and has a 42,860 m^2 array of fans supplying air at a velocity of 3.2 m/s in the interior of the air channels (or 2 m/s in the cross-section HxL), overcoming a ΔP of 114 Pa. The bricks have a residence time of approximately 807 h when assuming that 80% of the wall thickness carbonates in the air contactor (i.e., z_{carb} = 3.2 mm).

To satisfy the required volume for the proposed contactor design, the stacks of bricks were chosen to be 1.8 m^3 (1.8 × 1.0 × 1.0 m). This results in stacks of 20 × 8 × 4 hollow bricks as exhibited in Figure 3. Each brick has a width of 113 mm, a height of 78 mm, a length of 250 mm and contains six equally sized square holes of 27 mm (as illustrated in Figure 2). The gaps between bricks have the same equivalent diameter as the square holes, thus ensuring a homogeneous supply of CO_2 to the exposed solid surfaces of the bricks. These gaps may be formed, for example, by introducing small 14-mm-thick solid elements separating each brick (as shown in Figure 3).

The calculated residence time of the solids corresponds with an average brick movement of 0.012 m/h in a direction counter-current to the air flow. In the proposed contactor, the movement is achieved through intermittent displacement of the brick stacks (as shown in the bottom left of Figure 3) moved in the contactor using low-cost techniques widely available in similar industries (e.g., brick manufacture). We

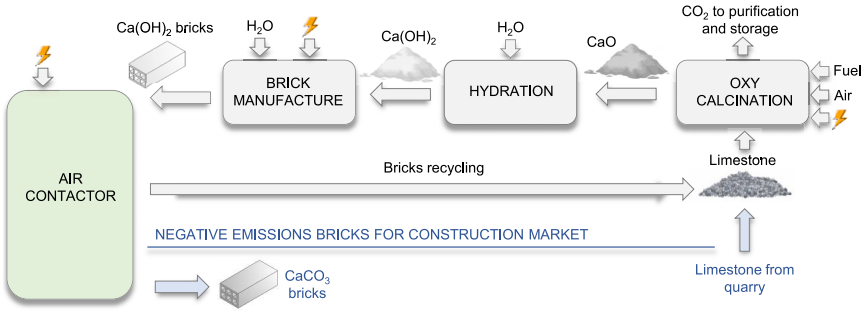

Figure 4. The full process to (re)generate the carbonated bricks upon leaving the DAC contactor
It consists of a closed calcium loop that includes destroying and recycling the carbonated bricks to extract the CO_2 by oxy-calcination. When the carbonated bricks are exported to the construction market to obtain a revenue that offsets the CO_2 capture cost (bottom) a continuous supply of limestone is required to manufacture the carbon-free bricks. In both cases, the CaO produced, either from recycled bricks or from fresh limestone, is hydrated to obtain a $Ca(OH)_2$ slurry that is then extruded in the form of the dry bricks used in the DAC contactor of Figure 3.

acknowledge that the shape of the stacks is today arbitrary, as this will depend on the final shape of the masonry units and their mechanical properties, in particular their crushing strength at the exit of the extrusion process that will determine the number of bricks that can be piled up on top of each other. Shelving of the bricks may be needed to overcome these limitations and we have assumed in the following section that the cost of these selves are negligible when compared with other major CAPEX cost components (see Table 3). It must be noted that the calculated average velocity of displacement is a result of the distance of each displacement being equivalent to the stack dimension in the direction of the airflow (i.e., 1 m). To increase the homogeneity of the carbonation process, the stacks may be rotated 180° with each displacement, thus exposing the stacks to air flows with maximum and minimum air concentrations. To fill the entire contactor, 231,883 stacks are required, each with a volume of 1.8 m^3. These stacks could be arranged over several floors, being the gap between the stacks and the floor minimized and/or covered by flexible flaps to block the passage of air to avoid channeling issues. To achieve the residence time adopted for this reference case, a 2.9 km/h stack displacement is required, which lies within the standard operating ranges for velocities of existing warehouse robots (i.e., 2–5 km/h). Therefore, the movement of the solids may be achieved using a single warehouse robot, with the brick stacks being in a stationary position most of the time, and displaced by just 1 m approximately once every 3 days. This slow motion also guarantees that the stacks are tightly packed at any point in time. Even if the movement of the stacks involved the creation of a full corridor empty of stacks, this will represent at any point in time less than 0.01% of the air contactor volume and will only last a small fraction of the residence time of the stacks in the air contactor.

Table 1 compiles the assumptions and design choices that make up the basic design of a system as outlined in Figure 3 (see Note S1 and Figures S1 and S2 for more details). This table is the basis for the cost analysis presented in the following section.

Cost analysis

The estimation of cost per ton of CO_2 captured from air requires the consideration of the full system, which, besides the air contactor described in the previous section, comprises the $CaCO_3$ oxy-calcination process and the manufacture of $Ca(OH)_2$

Table 2. Parameters used for cost calculations

Parameter	Units	FOAK	NOAK
Electricity price	$/MWh$_e$ ($/GJ$_e$)	68 (18.9)	50 (13.9)
Fuel price	$/MWh$_{th}$ ($/GJ$_{th}$)	19 (5.3)	8 (2.2)
Cost of capital (i)	%	10	5
Lifetime (n)	years	30	30
Capital recovery factor[a]	%	10.6	6.5

The values of the parameters used for the cost calculations as reported in this table have been taken from the IEAGHG report.[16]

[a]Calculated as $[i \cdot (1+i)^n/((i+1)^n-1)]$.

bricks (Figure 4). Basic cost assumptions for these operations are described and justified below. Reported CO_2 capture efficiencies do not account for the emissions associated with the electricity needed to run the DACCS system. The costs of the compression, transport, and storage of CO_2 are site dependent and may not be applicable when the CO_2 is used as a feedstock for synthetic fuels. However, to allow cost comparisons with other DACCS systems reviewed in a recent IEAGHG study on DACCS,[16] the same cost has been adopted for this component (20 $/t-$CO_2$, that can be decreased to 5 $/t-$CO_2$ if large capacity shared infrastructure is used alongside low-cost storage locations). The cost figures used below are only indicative and subject to uncertainty, contingencies, and site-specific assumptions (i.e., the availability of limestone, energy, and water at reasonable cost). Following the IEAGHG report,[16] and to analyze current and future cost of the DACCS system proposed, the estimation of cost per ton of CO_2 captured is here presented for a first-of-a-kind (FOAK) plant commissioning in mid-2020s and long-term nth-of-a-kind (NOAK) plant. Reference values of the main cost parameters (i.e., electricity and fuel prices, cost of capital, and lifetime of the plants) used for both cost calculations have been taken from this report[16] and are summarized in Table 2. All costs here reported are in 2020 U.S. dollars, being this year chosen to ensure a fair cost comparison with other DACCS systems previously reported and avoid the alteration of high inflation rates experienced since mid-2021. The use of further cost ranges and sensitivity analyses have been avoided, as they would introduce additional variability and arbitrary choices. The cost figures below obtained are supported by cost information on similar components used in large-scale industries or from emerging CO_2 capture and storage systems close to industrial-scale demonstration in the lime and cement sectors.

As presented in Figure 4, the main fate considered for the bricks is to recycle and destroy them to extract CO_2 by calcining the $CaCO_3$ formed in the air contactor. Under such conditions, a closed calcium loop requiring a negligible consumption of limestone is established. With this option, the extrusion step can be made simpler, as any shape given to the $Ca(OH)_2$ solids would be valid, so long as the pressure drop constraints referred to above are met.

The specific CO_2 capture cost is calculated following a methodology consistent with that applied to other emerging CO_2 capture systems.[34] Thus, the specific cost components of Table 3 are calculated as follows.

(1) Capital expenditure on equipment (CAPEX): As indicated in Table 2, an average capital recovery factor of 10.6% and 6.5% has been applied to FOAK and NOAK calculations, respectively. The highest cost in this category arises from the equipment needed for the calcination island, including the oxy-calciner, CO_2 compression and purification unit (CPU), air separation unit

Table 3. Summary of the costs of the main components of the proposed DACCS system

Cost component		Reference			$/t-$CO_2$ captured in the air contactor	
		Units	Value			
			FOAK	NOAK	FOAK	NOAK
Calcination island + CPU + CO_2 transport and storage	CAPEX Oxy-calciner, ASU, CPU and hydrator	M$	723	573	85.2	41.4
	CAPEX Brick manufacture		135	107	15.9	7.7
	fixed OPEX	M$/year	33.4	26.5	33.4	26.5
	variable OPEX: Fuel	GJ_{th}/t-CO_2	6.4	5.5	33.6	12.2
	variable OPEX: electricity ASU + CPU + Aux	MW_e	40		21.4	15.8
	variable OPEX: electricity brick manufacture	GJ_e/t-CO_2	0.6		10.7	7.9
	variable OPEX: process water cost	$/$m^3$	1	0.1	2.4	0.2
	CO_2 transport and storage	$/t-$CO_2$	20	5	20	5
	Subtotal				222.6	116.7
Air contactor	CAPEX structure	M$	85.3	42.6	10.1	3.1
	CAPEX fans		38.4	29.5	4.5	2.1
	CAPEX limestone batch	$/t-$CaCO_3$ (M$)	20 (6.3)	7 (2.2)	0.7	0.2
	fixed OPEX	M$/year	5.1	2.9	5.1	2.9
	variable OPEX: electricity	GJ_e/t-CO_2	0.4		7.9	5.8
	Subtotal				28.3	14.1
Total DACCS cost (without revenues from bricks)					250.9	130.8

All costs in 2020 US dollars.

(ASU), and hydration of the material. Considering the cost analysis performed by Keith et al.[12] and for the lime requirements in our system, the CAPEX of this equipment including the total project costs, would be estimated at around $361 million and $287 million for FOAK and NOAK plants, respectively, when applying a scale factor of 0.7. The IEAGHG technical report[16] suggested that a potential CAPEX of approximately twice these values is more realistic. Therefore, in our cost analysis CAPEX cost of $723 and $573 million for FOAK and NOAK plants have been considered, resulting in a contribution of 85.2 and 41.4 $/t-$CO_2$, respectively. These values are in agreement with our previous cost estimations for a FOAK plant[25] based on reference costs for oxy-combustion plants.[34]

Other contributors to the CAPEX consist of the brick manufacture equipment and the air contactor elements (structure and fans) costs. The brick manufacture equipment cost, has been calculated by scaling up the specific cost for similar operations reported by Youssef et al.[35] using their geopolymer brick production (i.e., without curing steps when compared to standard fired bricks), the CAPEX of the brick manufacture equipment is of $5.3 million for a production of 25,000 t/year.[35] In our proposed system, approximately 290 tons per hour of dry $Ca(OH)_2$ extruded are required to capture 1 Mt-CO_2/year in the air contactor. Using a scale factor of 0.7, this results in a cost of $135 million for FOAK plants, which account for approximately 16% of the CAPEX of the calcination island. The same cost ratio for the FOAK and NOAK systems as in the oxy-calciner island is used to estimate the brick manufacture equipment for a NOAK plant. These numbers are consistent with estimation costs provided by a vendor[36] that manufactures and commercializes machinery, equipment, services, and installations for materials extrusion at scales for single lines up to 400,000 t/year and equipment cost of about $3 million per machine. It must be noted that the extrusion machine represents approximately one-fourth of the capital expenditure for bricks manufacture (i.e., including mixing of solids, robotics to pile up the bricks, and conveying belts).

The air contactor structure cost was estimated assuming 400 and 200 $/m^2 flooring cost, respectively, for FOAK and NOAK plants. For the fans, the cost was estimated using the conservative capital cost assumptions of Holmes and Keith[28] for a DAC contactor operating under pressure drop requirements comparable with those of the contactor depicted in Figure 3, being approximately $38.4 million for a FOAK plant (30% higher than for a NOAK plant).

Finally, the capital expenditure for the first batch of material in the air contactor has been included in the cost analysis. Here, limestone costs of 20 and 7 $/t-$CaCO_3$ have been assumed for the FOAK and NOAK plants, which is consistent with the U.S. Geological Survey[37] data available for commodity crushed stone. As result, the contribution of the air contactor elements CAPEX (i.e., structure, fans and limestone) is just of 15.3 and 5.4 $/t-$CO_2$ for FOAK and NOAK plants, less than 15% of that of the calcination island. This is obviously a critical advantage with respect to alternative DAC systems: once the costs of producing de-carbonized $Ca(OH)_2$ are taking into account, the remaining cost components in the proposed DAC system are relatively minor cost contributors, subject to low contingencies.

(2) Fixed operational costs (Fixed OPEX): These include the fixed maintenance and labor OPEX (assumed to be 3% of the total CAPEX and 30% of the maintenance costs, respectively). As reported in Table 3, these contribute with about 38.5 and 29.4 $/t-$CO_2$ for FOAK and NOAK plants, respectively.

(3) Variable operational costs (Variable OPEX): Include the costs of fuel, electricity consumables, raw materials (i.e., limestone and water), and CO_2 transport and storage. The thermal energy requirements of the limestone calcination step are assumed to be 5 GJ_{th}/t-CaO (or 6.4 GJ_{th}/t-CO_2). Because of recent major developments made by lime equipment manufacturers,[38] oxy-fired lime kilns with an energy consumption as low as 4.3 GJ_{th}/t-CaO will soon be available, meaning that this assumption can be considered conservative. This is further supported by the estimations made by Carbon Engineering, where an optimistic 4.1 GJ_{th}/t-CO_2 is assumed for their oxy-fired calcination step.[12] Considering the fuel costs reported on Table 2, this results on 33.6 and 12.2 $/t-$CO_2$ for FOAK and NOAK plants. The elements contributing to electricity consumption in the calcination island are the electricity linked with the brick manufacture machinery (with 0.6 GJ_e/t-CO_2, considering a consumption of 69 kWh_e per ton of brikcs[35]) and with the oxy-combustion island (i.e., for the ASU, CPUs and auxiliaries, with 1.3 GJ_e/t-CO_2 – equivalent to 40 MW_e[12,25]). Concerning the latter, this can be reduced to 0.8 GJ_e/t-CO_2 if the ASU is replaced with electrolytic O_2.[39] For electricity costs of 18.9 and 13.9 $/$GJ_e$, as reported in Table 2, the total electricity consumption in the calcination island results in 32.1 and 23.6 $/t-$CO_2$, respectively. The cost of process water (required for the hydration of $Ca[OH]_2$ and the brick manufacture process) can be highly variable, with upper and lower bounds of 1 $/m^3 and 0.1 $/m^3 at the location of the plant[12] as reported in Table 3. In the case that the cost of water reaches the higher value, 15–20 $/t-$CO_2$ should be added to the variable OPEX costs under the most pessimistic conditions. These conditions may be present in arid locations with low levels of humidity in the air that would require not only water for the sorbent regeneration (as indicated in Figure 4), but also to humidify air entering the air contactor. As mentioned above, a CO_2 transport and storage cost of 5–20 $/t-$CO_2$[16] is included in the cost analysis. Concerning the variable OPEX in the air contactor, this includes mainly the electricity consumption of the fans (0.4 GJ_e/t-CO_2 as calculated in Note S1, see also Figure S3, which is equivalent to 13.3 MW_e).

As shown in Table 3, 251 and 131 $/t-$CO_2$ have been calculated for a FOAK and NOAK plants, respectively, being the calcination island, CPU, and CO_2 transport and storage the main elements contributing to the total cost. If reference cost numbers were taken as those reported by Carbon Engineering[12] (i.e., same oxy-calcination island CAPEX, fixed and variable OPEX costs, and capital recovery factors), the system proposed in this work would reach a NOAK cost of 108 $/t-$CO_2$, which is 12 $/t-$CO_2$ below the reference cost reported by Carbon Engineering[12] under the same assumptions (scenario with gas and electricity input).

By future research on the carbonated bricks, potential uses can be expected as construction materials. The added value of the bricks could translate into a breakthrough reduction in the DACCS cost analysis, at least for the FOAK demonstration systems. In this option (see Figure 4), there is a continuous supply of natural limestone delivered to the system to manufacture the $Ca(OH)_2$ bricks while generating a stream of CO_2 suitable for transport and permanent storage or use. Thus, an additional cost of 68.4 $/t-$CO_2$ needs to be taken into account because of the necessary continuous supply of limestone. In addition, we assume an additional cost of 30 $/t-$Ca(OH)_2$ extruded (i.e., 76 $/t-$CO_2$) linked to the possible need of additives and aggregates to provide the necessary properties to the bricks. Furthermore, we upgrade the oxy-calciner island cost (oversized considering the continuous flow of fresh limestone instead of recycled material) and CO_2 transport and storage cost (as 1.4 t-CO_2 are stored per t-CO_2 captured in the contactor). The DACSS cost for this option escalates to 410 $/t-$CO_2$ captured in the air contactor. However, this cost can be offset and brought to zero if it is possible to recover 0.2 $/brick in a FOAK plant. Therefore, the fact that two commodities (i.e., pure CO_2 and negative emissions bricks) can be produced in the DAC system, offers a competitive advantage for the early deployment of the proposed DAC technology.

EXPERIMENTAL PROCEDURES

Resource availability

Lead contact

Correspondence and requests for resources should be addressed to the lead contact, Yolanda A. Criado (yolanda.ac@incar.csic.es).

Materials availability

This study did not generate any new materials.

Data and code availability

The experimental evidence on carbonation rates of porous $Ca(OH)_2$ forms is presented in Criado and Abanades.[24] The design of the air contactor is based on the plug flow model used to estimate capture efficiencies and can be found in Note S1. Requests for further information should be sent to the lead contact.

SUPPLEMENTAL INFORMATION

Supplemental information can be found online at https://doi.org/10.1016/j.xcrp.2023.101339.

ACKNOWLEDGMENTS

This research is part of the CSIC program for the Spanish Recovery, Transformation and Resilience Plan (PTI+TRANSENER) funded by the Recovery and Resilience Facility of the European Union, established by the Regulation (EU) 2020/2094. The

authors would like to thank Carlos Serrano, from Talleres Felipe Verdés S.A., for the estimation of the extrusion equipment cost.

AUTHOR CONTRIBUTIONS

Conceptualization: J.C.A. and Y.A.C.; methodology: J.C.A. and Y.A.C.; investigation: Y.A.C. and H.I.W.; resources: Y.A.C. and H.I.W.; writing - original draft: J.C.A., Y.A.C., and H.I.W.; visualization: Y.A.C. and H.I.W.; supervision: J.C.A.; project administration: J.C.A.; funding acquisition: J.C.A.

DECLARATION OF INTERESTS

A European Patent Application (EP22382686) has been filed related to this work.

INCLUSION AND DIVERSITY

We support inclusive, diverse, and equitable conduct of research.

Received: November 25, 2022
Revised: February 17, 2023
Accepted: February 28, 2023
Published: March 21, 2023

REFERENCES

1. IPCC (2022). Climate Change 2022 - Mitigation of Climate Change. Summary for Policymakers. Working Group III Contribution to the Sixth Assessment Report of the Intergovernmental Panel on Climate Change.

2. Galán-Martín, Á., Vázquez, D., Cobo, S., Mac Dowell, N., Caballero, J.A., and Guillén-Gosálbez, G. (2021). Delaying carbon dioxide removal in the European Union puts climate targets at risk. Nat. Commun. *12*, 6490. https://doi.org/10.1038/s41467-021-26680-3.

3. IEA (2022). Direct Air Capture - A Key Technology for Net Zero (International Energy Agency).

4. Erans, M., Sanz-Pérez, E.S., Hanak, D.P., Clulow, Z., Reiner, D.M., and Mutch, G.A. (2022). Direct air capture: process technology, techno-economic and socio-political challenges. Energy Environ. Sci. *15*, 1360–1405. https://doi.org/10.1039/D1EE03523A.

5. Daggash, H.A., Fajardy, M., and Mac Dowell, N. (2020). Negative emissions technologies. In Carbon capture and storage, M. Bui and N. Mac Dowell, eds. (The Royal Society of Chemistry), pp. 447–511.

6. National Academies of Sciences Engineering and Medicine (2019). Negative Emissions Technologies and Reliable Sequestration: A Research Agenda (The National Academies Press). https://doi.org/10.17226/25259 GET.

7. Sanz-Pérez, E.S., Murdock, C.R., Didas, S.A., and Jones, C.W. (2016). Direct capture of CO_2 from ambient air. Chem. Rev. *116*, 11840–11876. https://doi.org/10.1021/acs.chemrev.6b00173.

8. Ramirez, A., Khamlichi, E., Markowz, G., Rettenmaier, N., Baitz, M., Jungmeier, G., and Bradley, T. (2020). LCA4CCU - Guidelines for Life Cycle Assessment of Carbon Capture and Utilisation (European Commission Directorate-General for Energy).

9. Müller, L.J., Kätelhön, A., Bachmann, M., Zimmermann, A., Sternberg, A., and Bardow, A. (2020). A guideline for life cycle assessment of carbon capture and utilization. Front. Energy Res. *8*, 15.

10. Sutter, D., van der Spek, M., and Mazzotti, M. (2019). 110th Anniversary: evaluation of CO_2-based and CO_2-free synthetic fuel systems using a net-zero-CO_2-emission framework. Ind. Eng. Chem. Res. *58*, 19958–19972. https://doi.org/10.1021/acs.iecr.9b00880.

11. Abanades, J.C., Rubin, E.S., Mazzotti, M., and Herzog, H.J. (2017). On the climate change mitigation potential of CO_2 conversion to fuels. Energy Environ. Sci. *10*, 2491–2499. https://doi.org/10.1039/C7EE02819A.

12. Keith, D.W., Holmes, G., St. Angelo, D., and Heidel, K. (2018). A process for capturing CO_2 from the atmosphere. Joule *2*, 1573–1594. https://doi.org/10.1016/j.joule.2018.05.006.

13. Leonzio, G., Fennell, P.S., and Shah, N. (2022). Analysis of technologies for carbon dioxide capture from the air. Appl. Sci. *12*, 8321. https://doi.org/10.3390/app12168321.

14. Climeworks (2022). Climeworks takes another major step on its road to building gigaton DAC capacity. https://climeworks.com/news/climeworks-announces-groundbreaking-on-mammoth.

15. House, K.Z., Baclig, A.C., Ranjan, M., van Nierop, E.A., Wilcox, J., and Herzog, H.J. (2011). Economic and energetic analysis of capturing CO_2 from ambient air. Proc. Natl. Acad. Sci. USA *108*, 20428–20433. https://doi.org/10.1073/pnas.1012253108.

16. IEAGHG (2021). Global Assessment of Direct Air Capture Costs (International Energy Agency Greenhouse Gas R&D Programme).

17. Herzog, H. (2022). Chapter 6 direct air capture. In Greenhouse Gas Removal Technologies (The Royal Society of Chemistry), pp. 115–137. https://doi.org/10.1039/9781839165245-00115.

18. Lackner, K.S., Grimes, P., and Ziock, H.J. (2001). Capturing carbon dioxide from air. In First National Conference on Carbon Sequestration (Department of Energy National Energy Technology Laboratory), pp. 1–15. Session 7B:Capture, V:Adsorption Studies.

19. Elliott, S., Lackner, K.S., Ziock, H.J., Dubey, M.K., Hanson, H.P., Barr, S., Ciszkowski, N.A., and Blake, D.R. (2001). Compensation of atmospheric CO_2 buildup through engineered chemical sinkage. Geophys. Res. Lett. *28*, 1235–1238. https://doi.org/10.1029/2000GL011572.

20. Nikulshina, V., Hirsch, D., Mazzotti, M., and Steinfeld, A. (2006). CO_2 capture from air and co-production of H_2 via the $Ca(OH)_2$–$CaCO_3$ cycle using concentrated solar power–Thermodynamic analysis. Energy *31*, 1715–1725. https://doi.org/10.1016/j.energy.2005.09.014.

21. Oates, J.A.H. (1998). Lime and Limestone: Chemistry and Technology, Production and Uses (Wiley-VCH). https://doi.org/10.1002/9783527612024.

22. Hanak, D.P., and Manovic, V. (2018). Combined heat and power generation with lime production for direct air capture. Energy Convers. Manag. *160*, 455–466. https://doi.org/10.1016/J.ENCONMAN.2018.01.037.

23. Erans, M., Nabavi, S.A., and Manović, V. (2020). Carbonation of lime-based materials under ambient conditions for direct air capture.

J. Clean. Prod. *242*, 118330. https://doi.org/10.1016/J.JCLEPRO.2019.118330.

24. Criado, Y.A., and Abanades, J.C. (2022). Carbonation rates of dry $Ca(OH)_2$ mortars for CO_2 capture applications at ambient temperatures. Ind. Eng. Chem. Res. *61*, 14804–14812. https://doi.org/10.1021/acs.iecr.2c01675.

25. Abanades, J.C., Criado, Y.A., and Fernández, J.R. (2020). An air CO_2 capture system based on the passive carbonation of large $Ca(OH)_2$ structures. Sustain. Energy Fuels *4*, 3409–3417. https://doi.org/10.1039/D0SE00094A.

26. Goff, A., Beauchamp, D., Fetvedt, J.E., Palmer, M.R., Lu, X., and Rathbone, D. (2021). Direct Capture of Carbon Dioxide. WO 2021/111366 A1.

27. Brandt, A.M. (2009). Cement-based Composites: Materials, Mechanical Properties and Performance, 2nd ed. (Taylor & Francis).

28. Holmes, G., and Keith, D.W. (2012). An air–liquid contactor for large-scale capture of CO_2 from air. Philos. Trans. A Math. Phys. Eng. Sci. *370*, 4380–4403. https://doi.org/10.1098/rsta.2012.0137.

29. Wilkinson, M.B., van der Spuy, J., and von Backström, T.W. (2017). The design of a large diameter axial flow fan for air-cooled heat exchanger applications. In Proceedings of the ASME Turbo Expo 2017: Turbomachinery Technical Conference and Exposition. Volume 1: Aircraft Engine; Fans and Blowers; Marine; Honors and Awards. https://doi.org/10.1115/GT2017-63331.

30. Klopfer, H. (1978). The carbonation of external concrete and how to combat it. Bautenschutz Bausanier *1*, 86–97.

31. Moorehead, D.R. (1986). Cementation by the carbonation of hydrated lime. Cem. Concr. Res. *16*, 700–708. https://doi.org/10.1016/0008-8846(86)90044-X.

32. Beruto, D.T., and Botter, R. (2000). Liquid-like H_2O adsorption layers to catalyze the $Ca(OH)_2$/CO_2 solid–gas reaction and to form a non-protective solid product layer at 20°C. J. Eur. Ceram. Soc. *20*, 497–503. https://doi.org/10.1016/S0955-2219(99)00185-5.

33. Klemm, W.A., and Berger, R.L. (1972). Accelerated curing of cementitious systems by carbon dioxide: Part I. Portland cement. Cem. Concr. Res. *2*, 567–576. https://doi.org/10.1016/0008-8846(72)90111-1.

34. Guandalini, G., Romano, M.C., Ho, M., Wiley, D., Rubin, E.S., and Abanades, J.C. (2019). A sequential approach for the economic evaluation of new CO_2 capture technologies for power plants. Int. J. Greenh. Gas Control *84*, 219–231. https://doi.org/10.1016/j.ijggc.2019.03.006.

35. Youssef, N., Lafhaj, Z., and Chapiseau, C. (2020). Economic analysis of geopolymer brick manufacturing: a French case study. Sustainability *12*, 7403. https://doi.org/10.3390/su12187403.

36. Serrano, C. (2023). Personal Communication (Talleres Felipe Verdés S.A.).

37. USGS (2022). Crushed stone statistics and information. https://www.usgs.gov/centers/nmic/crushed-stone-statistics-and-information.

38. Piringer, H., Bucher, P., and Wallimann, R. (2021). Sustainable lime burning technology with shaft kilns. ZKG Cem. Lime Gypsum, 34–41.

39. Davis, S.J., Lewis, N.S., Shaner, M., Aggarwal, S., Arent, D., Azevedo, I.L., Benson, S.M., Bradley, T., Brouwer, J., Chiang, Y.-M., et al. (2018). Net-zero emissions energy systems. Science *360*, eaas9793. https://doi.org/10.1126/science.aas9793.